

# Secondary Relaxation Processes in Polybutadiene Studied by $^2\text{H}$ Nuclear Magnetic Resonance and High-Precision Dielectric Spectroscopy

S. A. Lusceac, C. Gainaru, M. Vogel,<sup>†</sup> C. Koplin, P. Medick, and E. A. Rössler\*

Physikalisches Institut Experimentalphysik II, Universität Bayreuth, 95440 Bayreuth, Germany

Received January 5, 2005; Revised Manuscript Received March 18, 2005

**ABSTRACT:** Using  $^2\text{H}$  NMR and high-precision dielectric spectroscopy, we identified in polybutadiene (PB) at low temperatures (20–100 K) a third relaxation process ( $\gamma$ -process) in addition to the  $\alpha$ - and  $\beta$ -processes. PB samples with different molecular weights ( $M_w$ ) exhibit a strongly varying relaxation strength ( $\Delta\epsilon_\gamma$ ) though no clear-cut relationship is observed between  $\Delta\epsilon_\gamma$  and  $M_w$ . Concerning the temperature dependence of the  $\gamma$ -process, the set of samples can be divided into two subsets characterized by different activation energies, where one subset of time constants agrees well with those obtained recently from quasi-elastic light scattering in the melt. From our NMR experiments we conclude that at  $T < T_g$  a highly hindered motion ( $<8^\circ$ ) is responsible for the  $\gamma$ -process, which is difficult to explain by typical conformational changes.

## 1. Introduction

It is established that, in addition to the main relaxation ( $\alpha$ -process), polymers exhibit secondary relaxation processes that determine the relaxation behavior in the glassy state, i.e., below the glass transition temperature  $T_g$ .<sup>1–4</sup> Often these processes are attributed to motions of side groups or to conformational changes within the main chain. Hence, in the first place intramolecular potentials are expected to determine these relaxation processes, although, of course, an intermolecular contribution to the potentials may always be present. This is recognized when methyl group or phenyl ring rotation is considered.<sup>5–7</sup> In all cases a broad distribution of barrier heights is observed, reflecting the disordered environment of the reorienting group in the polymer glass.

Secondary relaxation processes, however, are also observed in low-molecular-weight glass formers composed of rigid molecules. A prominent example is toluene forming a glass with a pronounced secondary relaxation process.<sup>8</sup> Following the work of Johari and Goldstein<sup>9</sup> (JG), these processes are believed to be intrinsic to the glass, and they are often called JG  $\beta$ -processes. One may think that at least some of the secondary relaxation observed in polymers may be intrinsic JG, too. For example, there are polymers without side group, most prominently polybutadiene, which exhibits a strong JG  $\beta$ -process.<sup>8,10–14</sup> Clearly, monitoring a secondary relaxation process via a relaxing dipole moment in a side group does not allow one to conclude that the process is caused by the motion of the side group solely. For example, NMR has identified the  $\beta$ -process in PMMA as a  $180^\circ$  jump of the ester group that is coupled to a small-amplitude motion of the polymer chain.<sup>15–17</sup> Already Williams and Watts discussed the possibility that the intrinsic  $\beta$ -process attributed to the main chain may allow the side groups to reorient by large-amplitude motion.<sup>4</sup> Then one may ask whether the often coined term of a “local” motion is

still meaningful for secondary relaxations. Most of these processes are not of the type where a methyl or phenyl group rotates in a potential defined by the high symmetry of the group and where the term local motion indeed applies.

Regarding the nature of the intrinsic  $\beta$ -processes, two competing interpretations were offered. On one hand, Johari and Goldstein introduced the idea of “islands of mobility”, which survive in the glassy state and which contain a certain amount of mobile molecules.<sup>9</sup> On the other hand, Williams and Watts assumed that all molecules participate in the  $\beta$ -process performing small-amplitude reorientations which lead to a partial loss of the dielectric correlation function.<sup>4</sup> The concept of islands of mobility was applied to explain several experimental findings, but all the experiments trying to identify this fraction of mobile molecules in a sea of immobilized molecules failed so far. Instead, recent solvation<sup>18</sup> and NMR experiments<sup>19–24</sup> clearly demonstrated that essentially all the molecules participate in the JG process. Applying multidimensional techniques in the case of toluene, NMR shows that for most of the molecules the amplitude is close to  $4^\circ$  and somewhat less limited motion covering the range  $10^\circ$ – $90^\circ$  is possible only for 10–20% of the molecules.<sup>21–23</sup> Thus, molecules move in a spatially highly restricted way.

Currently, the JG  $\beta$ -process in molecular glass formers is intensively studied by several techniques.<sup>25</sup> A remarkable result recognized, in addition to the fact that essentially all molecules participate, is that its activation energy is often proportional to  $T_g$ , i.e.,  $E \approx 24T_g$ , though exceptions are reported.<sup>8,26,27</sup> Thus, the dynamics is nearly universal on the reduced temperature scale  $T/T_g$ . This holds also for the  $\beta$ -process of polybutadiene,<sup>8,23</sup> and indeed, the  $^2\text{H}$  NMR spectra close to  $T_g$  resemble that of toluene (cf. below). Another remarkable feature concerns the dielectric relaxation strength of the JG  $\beta$ -process. The relaxation strength strongly decreases while cooling above  $T_g$  but stays essentially constant below  $T_g$ .<sup>8,12,28</sup> Moreover, the temperature dependence of the time constants for the  $\beta$ -process may change when crossing  $T_g$ .<sup>26,29,30</sup> Any model for the  $\beta$ -process has to account for these features, and clearly, the behavior

<sup>†</sup> Institut für Physikalische Chemie, Westfälische Wilhelms-Universität Münster, Corrensstr. 30, D 48149 Münster, Germany.

\* Corresponding author. E-mail: ernst.roessler@uni-bayreuth.de.

cannot be explained within the framework of a simple thermally activated process.

For polymers further relaxation processes are observed<sup>5</sup> at temperatures well below  $T_g$ ,<sup>1</sup> which are termed  $\gamma$  and  $\delta$ , etc. However, little is known about the nature of these processes. One may speculate that, in contrast to the JG  $\beta$ -process, they may be attributed to polymer-specific features. In the case of polybutadiene (PB), indications for a third process were recently reported in a quasi-elastic light scattering study by Ding et al.<sup>31</sup> Already, Aouadi et al.<sup>32</sup> compiled a puzzling situation: different techniques, including Brillouin light scattering, dielectric spectroscopy, and neutron scattering,<sup>33</sup> reported quite different time constants, and they discussed the possibility of a “second  $\beta$ -process” with a smaller activation energy as that identified by dielectric spectroscopy. PB is also the subject of molecular dynamics simulation studies trying to identify the dynamics in the high-temperature melt.<sup>34,35</sup> Finally, we note that a picosecond relaxation process is found in all glass-forming systems including polymers, and its evolution is explained by mode coupling theory.<sup>36,37</sup>

Applying multidimensional NMR techniques secondary relaxation processes can be identified even in cases where the dielectric relaxation strength is very small.<sup>23</sup> In the present contribution we have extended our previous  $^2\text{H}$  NMR study of deuterated PB down to 80 K.<sup>23</sup> As we will show, indications for a further relaxation are found at low temperatures, and we will call it the  $\gamma$ -process. Moreover, we observe that guest molecules (benzene) in PB exhibit a similar  $\gamma$ -process as the neat polymer. In addition, we measured dielectric spectra down to low temperatures ( $>4$  K). Since PB has a small dipole moment, most commercially available spectrometers fail to monitor the dielectric loss of PB well below  $T_g$ . Here we used the Andeen Hagerling AH 2700 A high-precision capacitance bridge covering a frequency range from 50 to 20 000 Hz. We will demonstrate that also dielectric spectroscopy can identify a third relaxation process at low temperatures. Actually, indications of this process were already observed in measurements by Hansen and Richert<sup>10</sup> but not explicitly discussed. Our results for PB with different molecular weights will be compared with findings from other techniques. We will discuss the controversial results reported by various techniques.<sup>8,11,12,32,37,38</sup> Finally, we will use the NMR data to put severe constraints on the model designed to explain the secondary relaxation process in PB.

## 2. Theoretical Background

$^2\text{H}$  NMR spectroscopy probes the interaction between the electric quadrupole moment of the deuteron and the electric field gradient (EFG) present at the nucleus site. The EFG is generated by the charge distribution produced by the  $\text{C}-^2\text{H}$  bond. For the molecules used in our experiment the charge distribution is, to a good approximation, symmetric with respect to the  $\text{C}-^2\text{H}$  bond axis. In this case the NMR frequency (in the rotating frame) depends on the angle  $\theta$  between the bond direction and the external magnetic field:<sup>5</sup>

$$\omega(\theta) = \pm \frac{\delta}{2} [3 \cos^2(\theta) - 1] \quad (1)$$

where  $\frac{4}{3}\delta$  is the quadrupolar coupling constant. Thus, the rotational motion of the  $\text{C}-^2\text{H}$  bond is directly monitored by a change of  $\omega$ .

In a sample with an isotropic distribution of  $\theta$  angles (powder) and with absence of molecular motion the  $^2\text{H}$  NMR spectrum yields the shape of a Pake pattern.<sup>5,39</sup> The line shape changes when molecular motion takes place on the time scale of  $1/\delta \approx 10^{-5}$  s or faster. A particular case is encountered when the  $\text{C}-^2\text{H}$  bond reorients around a  $C_n$  axis ( $n > 2$ ) with a correlation time  $\tau_n \ll 1/\delta$  (fast motion limit) and an angle  $\chi$  (between the direction of the bond and the direction of the  $C_n$  axis). The resonance frequency, provided that the motion of the axis itself is in the slow motion limit, is<sup>5</sup>

$$\omega(\alpha) = \pm \frac{\delta}{2} [3 \cos^2(\alpha) - 1] \quad (2)$$

where  $\alpha$  is the angle between the  $C_n$  axis and the external magnetic field. The motional averaged spectral width reads

$$\bar{\delta}(\chi) = \frac{\delta}{2} [3 \cos^2(\chi) - 1] \quad (3)$$

Once again, the spectrum has the shape of a Pake spectrum, but the spectral width is reduced.

To measure the spectrum, one usually applies the solid-echo pulse sequence ( $90^\circ_x - t_p - 90^\circ_y$ ), where  $t_p$  is the time delay between the pulses. In the absence of molecular motion the time signal following the echo maximum is identical to the free induction decay (FID). On the other hand, when molecular motion is present, the  $t_p$  dependence of the spectral shape provides information about the angular amplitude and type of the motion.<sup>40,41</sup> This kind of experiment proves particularly valuable to detect angular motion that is highly restricted in space, and among others,<sup>42,43</sup> our group has applied the technique to study secondary processes in several glasses.<sup>20–23,41</sup> Because of the angular dependence of  $\omega(\theta)$  (cf. eq 1), the spectral intensity at zero frequency is most sensitive to the  $t_p$  increment.<sup>21,23</sup> More precisely, the central part of the spectrum decreases with increasing  $t_p$  much faster than the “singularities” of the Pake shape, so that the latter are the only surviving features at long  $t_p$  (cf. Figure 1). To quantify the  $t_p$ -related line-shape changes, we use the relative spectral intensity at zero frequency  $R(t_p, T)$ :

$$R(t_p, T) = \frac{1}{h} S(t_p, \omega = 0, T) \quad (4)$$

where  $S(t_p, \omega, T)$  is the spectrum measured with the interpulse delay  $t_p$  and  $h$  is the average “singularity” height:

$$h(t_p, T) = \frac{1}{2} [\max(S(t_p, \omega > 0, T)) + \max(S(t_p, \omega < 0, T))] \quad (5)$$

$h(t_p, T)$  was used instead of the maximum of the spectrum to account for the fact that measured spectra, in particular for long  $t_p$ , are usually slightly asymmetric (with respect to the  $\omega = 0$  axis) due to experimental artifacts. We emphasize that for glass formers that do not exhibit a secondary relaxation no line-shape changes are observed when varying  $t_p$  below  $T_g$ .<sup>23</sup>

In addition to NMR line-shape analysis there are other NMR methods to study secondary relaxation processes. For example, the spin–lattice relaxation rate  $1/T_1$  is related to the spectral density  $J^{(2)}$  of the molec-

ular motion. One should note that in the glassy state ( $T < T_g$ ) the spin–lattice relaxation function is usually nonexponential due to a broad distribution of correlation times, and therefore the mean relaxation rate  $\langle 1/T_1 \rangle$  has to be considered.<sup>6</sup> Assuming that the EFG tensor is axially symmetric, for powder samples one gets the following equation:<sup>44</sup>

$$\left\langle \frac{1}{T_1} \right\rangle \propto J^{(2)}(\omega_0) + 4J^{(2)}(2\omega_0) \quad (6)$$

with  $\omega_0$  being the Larmor frequency. The spectral density  $J^{(\lambda)}$  is described by<sup>44</sup>

$$J^{(\lambda)}(\omega) = \frac{1}{2} \operatorname{Re} \left( \int_{-\infty}^{\infty} \phi^{(\lambda)}(t) e^{i\omega t} dt \right) \quad (7)$$

where  $\phi^{(\lambda)}(t)$  is the normalized reorientation autocorrelation function of rank  $\lambda$ .

In theory, the relaxation rate  $\langle 1/T_1 \rangle$  can be obtained from the initial slope of the spin–lattice relaxation function.<sup>44</sup> In practice, more reliable relaxation data are obtained taking the average spin–lattice relaxation time  $\langle T_1 \rangle$  by performing the integral over the normalized spin–lattice relaxation function  $f(t)$ . Explicitly, we fit the relaxation function with  $f(t) = \exp[-(t/\tau)^\beta]$  and calculated the average spin–lattice relaxation time according to  $\langle T_1 \rangle = (\tau/\beta)\Gamma(1/\beta)$ , where  $\Gamma$  is the gamma function.<sup>6</sup> Below  $T_g$  the proportionality  $\langle T_1 \rangle \propto \langle 1/T_1 \rangle^{-1}$  holds in good approximation.<sup>44</sup>

In dielectric spectroscopy, the dipole autocorrelation function  $\phi^{(1)}(t)$  is probed provided that cross-correlation effects can be neglected.<sup>3</sup> For the imaginary part of the permittivity  $\epsilon''(\omega)$  the relation

$$\frac{\epsilon''(\omega)}{\Delta\epsilon} = \omega J^{(1)}(\omega) \quad (8)$$

holds, where  $\Delta\epsilon$  is the relaxation strength.

### 3. Experimental Details

For the  $^2\text{H}$  NMR experiments we used 1,4-polybutadiene- $d_6$  (PB- $d_6$ ,  $M_w = 80\,000$  g/mol, courtesy of D. Richter) previously employed for our studies<sup>21,23,45</sup> and 9.4 wt % benzene- $d_6$  in 1,4-polybutadiene (PB-777,  $M_w = 777$  g/mol). Benzene- $d_6$  was purchased from Sigma-Aldrich and PB-777 from Polymer Standard Service (Mainz, Germany). Both compounds were used without further purification. The spectra were measured applying a solid-echo pulse sequence preceded by a saturation sequence (five  $90^\circ$  pulses). We chose a time period  $t_d$  between the saturation and the solid-echo sequences such that more than 95% of the equilibrium magnetization is probed. For the sample PB- $d_6$  a Bruker CXP 200 spectrometer equipped with a TecMAG data acquisition system was used, and for the 9.4% benzene- $d_6$  in PB-777 sample a Bruker DSX 400 spectrometer was used. For both spectrometers, the same superconductive magnet was employed, providing a  $^2\text{H}$  Larmor frequency of 46.07 MHz. The samples were placed in a home-built low-temperature probe inserted in an Oxford static cryostat CF 1200, providing a temperature stability better than 0.2 K. The pulse lengths for the  $90^\circ$  pulse was about 2.3  $\mu\text{s}$  for PB- $d_6$  and 2.7  $\mu\text{s}$  for benzene- $d_6$ . The spin–lattice relaxation time was measured by applying the saturation recovery sequence.

In the dielectric experiments the following protonated samples were measured: 1,4-polybutadiene with  $M_w = 577$  g/mol (PB-577),  $M_w = 777$  g/mol (PB-777),  $M_w = 1450$  g/mol (PB-1450),  $M_w = 2010$  g/mol (PB-2010),  $M_w = 11\,400$  g/mol (PB-11400),  $M_w = 19\,900$  g/mol (PB-20000), and  $M_w = 87\,000$  g/mol (PB-87000). All samples were purchased from Polymer Standard Service and used as received. To find the concentra-

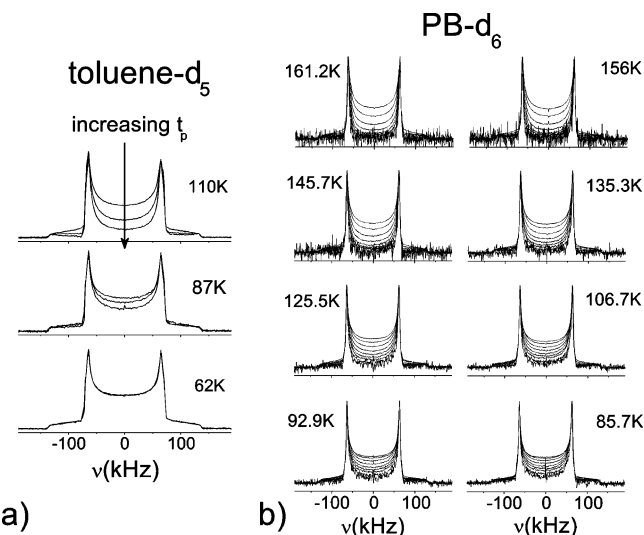


**Figure 1.** Normalized solid-echo spectra as a function of solid-echo pulse delay  $t_p$  at different temperatures for (a) toluene- $d_5$ .  $t_p$  values are 20, 100, and 200  $\mu\text{s}$  for the two highest temperatures and 20 and 200  $\mu\text{s}$  for 62 K. (b) Corresponding spectra for 1,4-polybutadiene- $d_6$  (PB- $d_6$ ).  $t_p$  values are 20, 50, 100, 150, 200, 250, 300, 400, and 500  $\mu\text{s}$ . For both pictures, the larger the area of the spectrum, the smaller is  $t_p$ .

tion of cis, trans, and vinyl units in the samples, a  $^{13}\text{C}$  high-resolution study was performed on PB-777, PB-2010, PB-11400, PB-19900, and PB-87000. The used spectrometer was Unity Inova 400 NB high-resolution NMR system with a probe  $^1\text{H}/^{19}\text{F}/^{31}\text{P}/^{13}\text{C}$  5 mm. One representative spectrum (Figure 11) and a figure with the obtained concentration values (Figure 12) are presented in the Appendix. The trans concentration is roughly constant disregarding molecular mass  $M_w$  ( $\approx 50\%$ ). On the other hand, the cis concentration is slightly decreasing with decreasing  $M_w$  from around 40% until more than 30% at the lowest measured  $M_w$ . Correspondingly, the vinyl content is increasing with decreasing molecular mass from roughly 10% to 20%.

In addition, a sample with  $M_w = 25\,000$  g/mol (PB-25000) and 7% vinyl manufactured by Scientific Polymer Products Inc. was investigated (courtesy of A. P. Sokolov) since a light scattering study was done by Ding et al.<sup>31</sup> on this polymer. For the high-precision dielectric measurements an Andeen Hagerling AH 2700 A high-precision capacitance bridge was employed. The instrument covers a frequency range from 50 to 20 000 Hz with a resolution  $\tan(\delta) \geq 2 \times 10^{-6}$ . Broad-band dielectric measurements were additionally performed in several cases. They were done using a Schlumberger SI 1260 phase gain amplifier together with a BDC current-to-voltage converter from Novocontrol. The setup provided a frequency range from  $10^{-3}$  to  $10^7$  Hz. The samples were placed in an Oxford CF 1200 dynamic cryostat, and a temperature stability better than 0.2 K was achieved. We took advantage of the design proposed by Wagner and Richert<sup>46</sup> in constructing the sample cell made of gold plated Invar steel to provide thermal invariance of the geometric capacitance ( $C_0 \approx 30$  pF).

### 4. Results

**4.1. NMR Measurements.** As discussed in the theoretical section, the presence of secondary processes can be revealed by measuring  $t_p$ -dependent solid-echo  $^2\text{H}$  NMR spectra.<sup>20–23</sup> The NMR results presented here are an extension of our previous work on polybutadiene.<sup>23,41,45</sup> To demonstrate the capability of such experiments, we first summarize our previous  $^2\text{H}$  NMR results for toluene, which exhibits a strong  $\beta$ -process as revealed by dielectric spectroscopy (DS). In Figure 1a we present solid-echo spectra of toluene- $d_5$  measured below  $T_g = 117$  K, normalized to their maximum value. At  $T$

$= 110$  K the spectrum for  $t_p = 20 \mu\text{s}$  is essentially given by a Pake spectrum. However, with increasing  $t_p$  the line shape changes: the central region of the spectrum decreases with respect to the height of the “singularities”. This line shape change is typical of small angle fluctuations which can be probed only for long  $t_p$  values.<sup>23,41</sup> Upon cooling the line-shape effects become smaller, and finally at  $T \approx 1/2 T_g$  the spectra for different values of  $t_p$  are indistinguishable and described by a Pake spectrum. To account for these experimental findings, one should keep in mind that the relaxation strength of the  $\beta$ -process is essentially constant below  $T_g$ , as proven by dielectric spectroscopy.<sup>8</sup> Then we can explain the temperature dependence of the solid-echo spectra by the shift of the distribution  $G_\beta(\ln \tau)$  through the experimental time window. While close to  $T_g$  the  $\beta$ -process lies right in the time window of the line shape analysis (microsecond time scale), it is too slow to be probed by the spectra at  $T = 1/2 T_g$ . This is in agreement with what is expected from the temperature dependence of  $G_\beta(\ln \tau)$  revealed by DS.<sup>8</sup>

From DS experiments it is known that the  $\beta$ -processes of PB and toluene show similar features;<sup>23</sup> i.e., the same activation energy  $E_a/T_g$ , a comparable prefactor, and a similar relaxation strength with respect to that of the  $\alpha$ -process are found. Therefore, we performed the same  $^2\text{H}$  NMR experiments for PB- $d_6$  with molecular weight  $M_w = 80\,000$  g/mol, and the results are presented in Figure 1b. Once again we measured below  $T_g = 181$  K.<sup>45</sup> The spectra observed at  $T = 161.2$  K are similar to those for toluene- $d_5$  slightly below  $T_g$ , indicating that they are typical of the  $\beta$ -process. However, unlike the line shape for toluene, the  $t_p$  dependence of the spectra does not change in a significant manner when lowering the temperature. At  $T = 86$  K ( $T < 1/2 T_g$ ) line shapes for various  $t_p$  values are still clearly different. Thus, on the  $T/T_g$  scale, the PB- $d_6$  spectra show a different dependence than those of toluene. While the features of the solid-echo spectra of PB- $d_6$  close to  $T_g$  can be explained as a consequence of the  $\beta$ -process, those at lower temperatures cannot since the  $\beta$  relaxation is already too slow to cause line shape changes, as shown by DS. Hence, the  $t_p$  dependence at, say,  $T \leq 1/2 T_g$  can only be rationalized by the presence of an additional motional process with a time constant much shorter than that of the  $\beta$ -process. We will call this relaxation process the  $\gamma$ -process.

To quantify the changes in the solid-echo spectra, we present in Figure 2 the quantity  $R(t_p, T)$  (see Theoretical Background), measuring the relative spectral intensity at  $\omega = 0$ . At a given temperature,  $R(t_p)$  is determined by the angular amplitude of the motion and its time constant  $\tau$ . Simulations have shown that  $R(t_p)$  decays the faster the larger the angle, and regarding  $\tau$ , the decay is fastest when  $\tau = 1/\delta \approx 10^{-5}$  s. For toluene- $d_5$  near  $T_g$  there is a large difference between the values of  $R(20 \mu\text{s}, 110 \text{ K})$  and  $R(200 \mu\text{s}, 110 \text{ K})$  that results from the  $\beta$ -process. With lowering the temperature this difference decreases and reaches zero at  $T \approx 1/2 T_g$ , indicating that the  $\beta$ -process exited the time window of the experiment. When inspecting the  $R$  values for PB- $d_6$ , we see that the difference  $R(20 \mu\text{s}, 161.2 \text{ K}) - R(200 \mu\text{s}, 161.2 \text{ K})$  close to  $T_g$  is similar to that of toluene, reflecting again the  $\beta$ -process. However, even at the lowest temperature,  $R(20 \mu\text{s}, 85.7 \text{ K}) \neq R(200 \mu\text{s}, 85.7 \text{ K})$ ; i.e., a strong  $t_p$  dependence of the line shape is

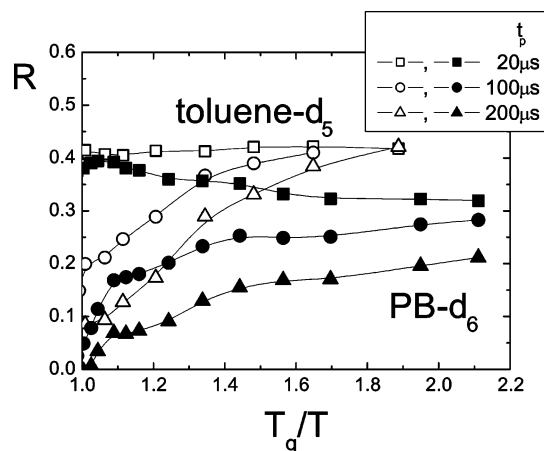


**Figure 2.** Relative spectral intensity at zero frequency  $R$  (cf. eq 4) for toluene- $d_5$  and PB- $d_6$ ; three solid-echo pulse delays  $t_p$  are considered. Lines are guides for the eye.

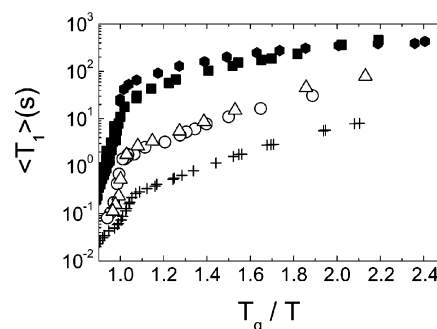


**Figure 3.** Mean spin-lattice relaxation times  $\langle T_1 \rangle$  for some glass formers as a function of reduced reciprocal temperature  $T_g/T$ : full squares, glycerol- $d_5$ ;<sup>47</sup> full hexagons, *o*-terphenyl- $d_{14}$ ;<sup>48</sup> open circles, toluene- $d_5$ ; open triangles, 45% chlorobenzene- $d_5$  in decalin; plus signs, 1,4-polybutadiene- $d_6$ .

observed. This different behavior has to be attributed to the presence of the  $\gamma$ -process.

Information about molecular motion can also be extracted from measurements of the spin-lattice relaxation.<sup>5,49</sup> In Figure 3 we present the temperature dependence of the mean spin-lattice relaxation time  $\langle T_1 \rangle$  for several glass formers. Focusing on temperatures well below  $T_g$ , we see that for glycerol- $d_5$  and *o*-terphenyl- $d_{14}$  (OTP- $d_{14}$ ), which do not exhibit a  $\beta$ -peak but only the excess wing,<sup>8,46</sup>  $\langle T_1 \rangle$  is significantly longer than for the other glasses. We mention that whether the excess wing is a kind of a JG  $\beta$ -process is currently debated.<sup>25,26,50,51</sup> Regarding toluene- $d_5$  and 45% chlorobenzene- $d_5$  in decalin, which display a  $\beta$ -process,<sup>8,23</sup>  $\langle T_1 \rangle$  is by more than an order of magnitude shorter than that of OTP- $d_{14}$ , for example. The difference can be rationalized by eq 6: at  $T < T_g$  the spectral density  $J^{(2)}(\omega_0)$  is much larger in systems that exhibit a  $\beta$ -process than in those without one. For PB- $d_6$  the  $\langle T_1 \rangle$  values are even an order of magnitude smaller than those for toluene- $d_5$  and chlorobenzene- $d_5$  in decalin. This indicates an even larger spectral density, corroborating our conclusion that an additional process exists in PB.

**4.2. Dielectric Spectroscopy Measurements.** A straightforward way to study whether a third relaxation process exists in PB is to perform dielectric spectroscopy (DS) experiments. However, the small electric dipole moment of PB hampers such investigation for most experimental setups. Up to our knowledge no systematic low-temperature PB dielectric study exists. We note that

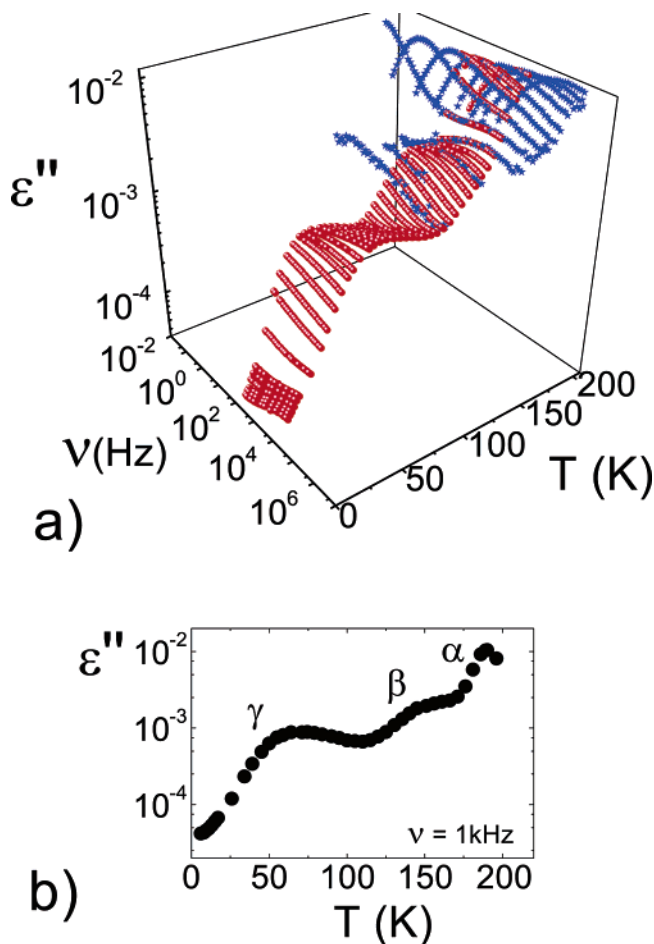


**Figure 4.** Imaginary part  $\epsilon''$  of the complex permittivity for 1,4-polybutadiene: (a) as a function of frequency  $\nu$  and temperature  $T$ ; blue stars, broad-band data<sup>8</sup> ( $M_w = 20\,000$  g/mol); red points, high-precision bridge data ( $M_w = 19\,900$  g/mol). (b) Dependence of  $\epsilon''$  on temperature at fixed frequency  $\nu = 1$  kHz.

in a paper by Hansen and Richert<sup>10</sup> indication of a such a process were presented but neither analyzed nor discussed. Therefore, initiated by our <sup>2</sup>H NMR findings, we performed a dielectric study in which the Andeen Hagerling high-precision bridge (cf. Experimental Details) was used in order to extend the accessible range of permittivity and to measure down to low temperatures.

In Figure 4a the imaginary part  $\epsilon''$  of the complex permittivity is presented for two samples: PB with  $M_w = 19\,900$  g/mol studied with the high-precision bridge and PB with  $M_w = 20\,000$  g/mol used in former broad-band experiments.<sup>8</sup> They have very similar molecular weights so that we will call them both PB-20000 in the following. Inspecting the broad band data, we see the main relaxation ( $\alpha$ -peak) at high temperatures. With lowering temperature the peak shifts to lower frequency, and a secondary peak ( $\beta$ -process) becomes visible. This  $\beta$ -peak is the only feature observed at the lowest temperature (around  $T = 130$  K) in the broad-band spectrum where the signal reaches the resolution limit of the setup  $\tan(\delta) \approx 10^{-3}$ . The covered spectral width of the high-precision measurements is smaller than that of the former experiment, but the improvement in  $\epsilon''$  resolution is obvious. Both data sets overlap at high temperatures. Below  $T = 100$  K a new relaxation feature (a third peak) enters the experimental frequency window. In Figure 4b, where  $\epsilon''(\nu = 1 \text{ kHz})$  vs  $T$  is

displayed, this third relaxation peak is clearly recognized. These results prove that, in addition to the  $\alpha$ - and  $\beta$ -process, a third process is present in PB-20000. Examining the temperatures as well as the time window in which the NMR line shape effects are observed, we conclude that dielectric spectroscopy and NMR measure the same  $\gamma$ -process at low temperatures.

In the hope to improve our understanding of the nature of the  $\gamma$ -process, PB samples with different molecular masses were investigated: PB-577, PB-777, PB-1450, PB-2010, PB-11400, PB-25000, and PB-87000 (see Experimental Details).

In Figure 5a,b the dielectric spectra  $\epsilon''(\nu)$  for PB-577 and PB-2010 are displayed. Once again, broad-band spectroscopy data are shown together with high-precision bridge data. The  $\gamma$ -process is discernible around 85 K for PB-577 and as a clear peak around 73 K in PB-2010. Even a fourth peak is observable at very low temperatures close to 4 K, but the low-temperature regime is not the subject of the present paper. Once again, these spectra demonstrate the extension of the accessible  $\epsilon''$  vs temperature range available. In Figure 5c we present  $\epsilon''(\nu = 1 \text{ kHz})$  as a function of temperature for different polymers. For all samples a  $\gamma$ -process is evident. To compare the polymers, the spectra normalized to their maximum value are plotted in Figure 5d. The processes mentioned so far are recognized: the  $\alpha$ -process ( $160 \text{ K} < T < 200 \text{ K}$ ), the  $\beta$ -process ( $125 \text{ K} < T < 160 \text{ K}$ ) and the  $\gamma$ -process at temperatures smaller than 125 K. We conclude that the  $\gamma$ -process is present in PB independent of the molecular weight. However, regarding the temperature dependence of the  $\gamma$ -process two groups can be distinguished: for PB-1450, PB-2010, PB-11400, and PB-20000 the peak lies around 60 K while for PB-577, PB-777, PB-25000, and PB-87000 it is found roughly 20 K higher. No systematic relation with the molecular weight shows up. For convenience, we will denote the first group  $\gamma_B$ -PB and the second one  $\gamma_A$ -PB. To illustrate the presence of two groups of PB, data for a member of each group are presented in Figure 6. Clearly, the  $\gamma$ -process manifests at different temperatures. Moreover, it is obvious that the  $\gamma$ -process is much broader than a Debye process.

While the relaxation strength of the  $\beta$ -process relative to that of the  $\alpha$ -process is only slightly altered, that of the  $\gamma$ -process strongly varies for the various polymers. For example, the value of  $\epsilon''(1 \text{ kHz})/\epsilon''_{\max}(1 \text{ kHz})$  for the  $\gamma$ -process is roughly the same for all the  $\gamma_A$ -PB, and it is by almost 2 orders of magnitude smaller than the value for the  $\alpha$ -process. In the group  $\gamma_B$ -PB, with augmenting molecular weight, the peak height is continuously increasing for PB-1450, PB-2010, and PB-20000. The sample PB-11400 is singular manifesting the strongest  $\gamma$ -process, with an amplitude of the peak of only a factor 3 smaller compared to that of the  $\alpha$ -process. However, again no systematic dependence on molecular weight is found in both  $\gamma_A$ -PB and  $\gamma_B$ -PB groups. Generally we found the relation  $\Delta\epsilon_{\gamma B}/\Delta\epsilon_{\alpha} > \Delta\epsilon_{\gamma A}/\Delta\epsilon_{\alpha}$ .

Spectra for which the  $\gamma$ -peak was clearly discernible were fitted with a log Gauss function  $G(\ln \nu)$ . From the frequency shift of the maximum  $\nu_{\gamma}$  we estimated the time constant of the  $\gamma$ -process as  $\tau_{\gamma} = 1/(2\pi\nu_{\gamma})$ . Because of the narrow frequency window of the high-precision bridge, a more advanced approach is not possible. For the low molecular weight samples (PB-577, PB-777) a quantitative analysis is hampered by a not well-resolved

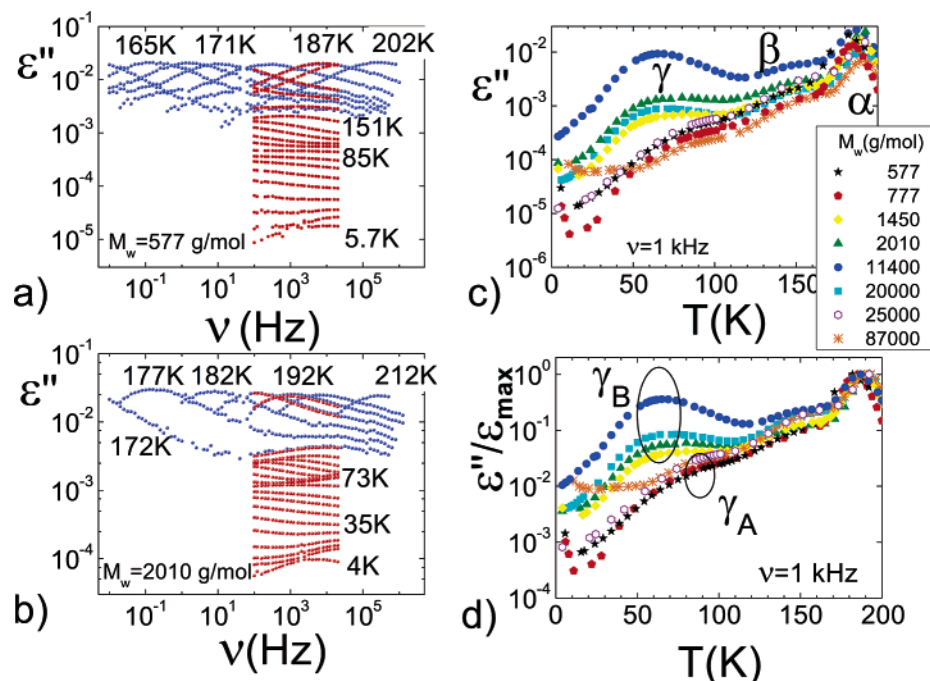


**Figure 5.**  $\epsilon''$  of polybutadiene (PB) as a function of frequency  $\nu$  for two different molecular weights: (a)  $M_w = 577$  g/mol and (b)  $M_w = 2010$  g/mol. Blue symbols, broad-band data; red symbols, high-precision data; some temperatures are indicated. (c)  $\epsilon''(1$  kHz) vs temperature  $T$  for PB samples with indicated molecular weight. (d) As in (c) but normalized  $\epsilon''(1$  kHz)/ $\epsilon''_{\max}(1$  kHz) vs  $T$ . Ellipses indicate different groups of  $\gamma$ -processes.

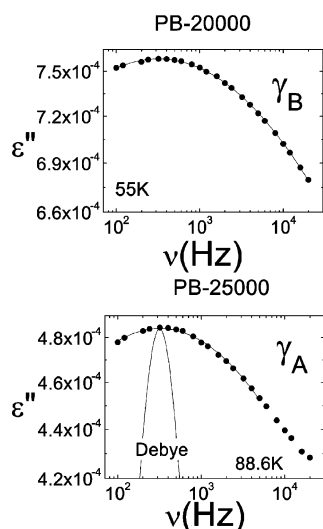


**Figure 6.** Dielectric spectra (on linear scale) for two polybutadiene samples (PB-20000 and PB-25000). The maximum of the  $\gamma$ -peak passes through the frequency window at different temperatures. Line is log Gauss fit. A Debye curve is displayed for comparison.

$\gamma$ -peak. In Figure 7a we present the time constants  $\tau_\gamma$  as a function of the reciprocal temperature for the polymers with  $M_w \geq 1450$  g/mol. Among each group the time constants of the  $\gamma$ -process are very similar, and they exhibit a thermally activated behavior. Fits with an Arrhenius law ( $\tau_\gamma = \tau_0 \exp(E/RT)$ ) provide mean activation energies  $E$  that are separated into two groups corresponding to the  $\gamma_A$ - and  $\gamma_B$ -PB. The range for  $\gamma_B$ -PB reads  $11 < E_{\gamma_B} < 14$  kJ/mol, and the values for  $E_{\gamma_A}$  are 17.5 and 20 kJ/mol (cf. Figure 7b). The prefactors  $\tau_0$  are in the range  $-13.5 < \log[\tau_0$  (s)]  $< -16.5$  (cf. Figure 7c).

In Figure 8 the time constants for the processes discussed so far are presented along with light scattering (LS) data on PB-25000 from Ding et al.<sup>31</sup> For

different molecular weights the curves  $\tau_\alpha$  vs  $1/T$  for the  $\alpha$ -process have essentially the same temperature dependence. They are slightly shifted because  $T_g$  is somewhat different. The time constants for the  $\beta$ -process show an Arrhenius temperature dependence with a somewhat different activation energies; note that  $E_\beta/T_g \cong \text{constant}$  is expected to hold.<sup>8,26,27</sup> Regarding the  $\gamma$ -process, one can see that it is well separated from both  $\alpha$ - and  $\beta$ -processes. Inspecting the LS and DS data for the  $\gamma_A$ -PB class, it is tempting to assume that the same process is probed though in quite different temperature ranges (as suggested by the straight line interpolation).

**4.3. Benzene- $d_6$  as a Guest in Polybutadiene.** To further investigate the  $\gamma$ -process, we studied a mixture of 9.4% benzene- $d_6$  in PB-777 by NMR. This polymer belongs to the  $\gamma_A$ -PB group. The question was whether and to what extent a guest molecules participate in the  $\gamma$ -process.

The corresponding solid-echo spectra measured at temperatures below  $T_g = 164$  K for various interpulse delays  $t_p$  are displayed in Figure 9a. For all  $T$ , the line shape strongly depends on  $t_p$ , indicating molecular motion in the experimental time window. The spectral width for benzene- $d_6$  is reduced because this molecule shows a specific fast rotation around its  $C_6$  axis (see eq 3).<sup>5</sup> Therefore, the  $t_p$  dependence of the spectra in Figure 9 probes the reorientation of the  $C_6$  axis rather than that of the C- $^2$ H bond.

To compare the findings in the mixture with those in neat PB, in Figure 9b a set of spectra for both benzene- $d_6$  in PB-777 and PB- $d_6$  are presented at the same reduced temperature  $\sim T_g/2$ . (PB- $d_6$  has its molecular weight close to the sample PB-87000 that belongs to the  $\gamma_A$ -PB group.) Clearly, the spectra are similar. Although the effects are a little more pronounced in neat PB- $d_6$ , the benzene- $d_6$  molecules show similar behavior as the host polybutadiene; this is also seen when the  $R$  values are compared (see Figure 9c). We conclude that the

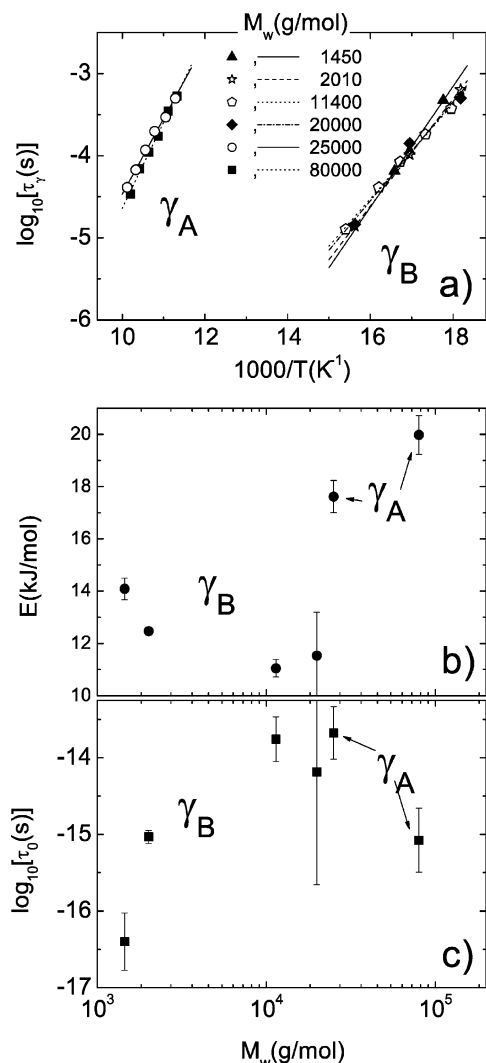


**Figure 7.** (a) Time constants  $\tau_\gamma$  of  $\gamma$ -process for different molecular weight ( $M_w$ ) polybutadiene samples; lines are Arrhenius fits. (b) Activation energy  $E$  vs  $M_w$ . (c) The prefactor  $\tau_0$  vs  $M_w$ .

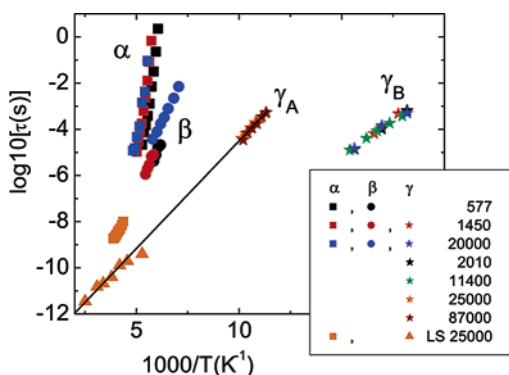


**Figure 8.** Time constants for the various processes in PB: squares,  $\alpha$ -process; circles,  $\beta$ -process; stars,  $\gamma$ -process. Light scattering (LS) data from Ding et al.<sup>31</sup> squares,  $\alpha$ -process; triangles, the extra relaxational process. Straight line is an Arrhenius interpolation.

motion of the benzene molecules and the motion of the PB segments are similar.

## 5. Discussion

Both  $^2\text{H}$  NMR and dielectric spectroscopy (DS) on 1,4-polybutadiene (PB) reveal that, in addition to the  $\alpha$ - and

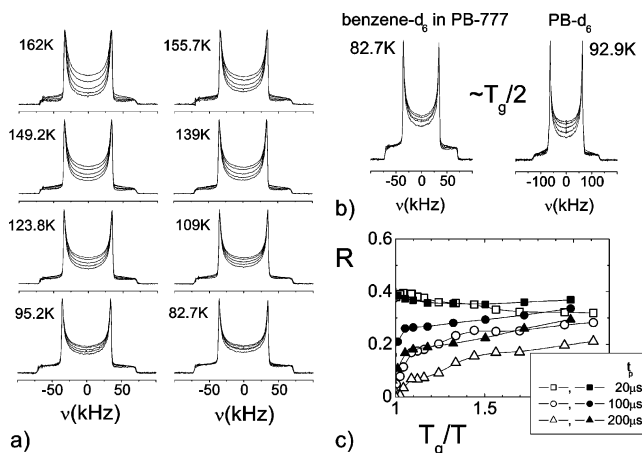


**Figure 9.** (a) Normalized solid-echo spectra at different temperatures for a 9.4% benzene- $d_6$  in 1,4-polybutadiene with  $M_w = 777$  g/mol (benzene- $d_6$  + PB-777); solid echo-pulse delays  $t_p$ : 20, 50, 100, 150, and 200  $\mu\text{s}$ , the smaller is  $t_p$ , the larger the area of the spectrum. (b) Comparison between benzene- $d_6$  + PB-777 and neat 1,4-polybutadiene- $d_6$  (PB- $d_6$ ,  $M_w = 80\,000$  g/mol) at  $T \approx T_g/2$ ;  $t_p$  values are the same as in (a). (c) Comparison of corresponding  $R$  values (cf. eq 4); closed symbols, benzene- $d_6$  + PB-777; open symbols, PB- $d_6$ . Lines are guides for the eye.

$\beta$ -processes, a third process is present, which is called the  $\gamma$ -process in this paper. It shows the following features: (i) The  $\gamma$ -process is significantly broader than a Debye process. (ii) The time constants of the process exhibit an Arrhenius temperature dependence; two groups of polymers can be distinguished according to the temperature dependence of their time constants. Within each group ( $\gamma_A$ -PB or  $\gamma_B$ -PB) a similar activation energy is found. (iii) The relaxation strength  $\Delta\epsilon_\gamma$  varies strongly for the different polymers; no clear-cut dependence on  $M_w$  or on the concentration of cis, trans, and vinyl units is found (cf. Appendix). The relation  $\Delta\epsilon_{\gamma_B} > \Delta\epsilon_{\gamma_A}$  is discovered. (iv) Benzene as a guest molecule in PB participates in the  $\gamma$ -process. Compiling the properties of the  $\gamma$ -process, we believe it is an intrinsic property of the PB polymers. We emphasize that we see no indication for both  $\gamma_A$  and  $\gamma_B$  being present simultaneously. Thus, we assume tentatively that they have the same origin but different activation energies.

There are several studies about processes other than  $\alpha$  or  $\beta$  for PB, most of them focusing on the dynamics in the melt. For example, Kanaya et al.,<sup>52</sup> performing a neutron scattering study, report, in addition to the  $\alpha$ -process, a process with an activation energy of  $E \sim 10.5$  kJ/mol. Aouadi et al.<sup>32</sup> applying Brillouin scattering, found an activation energy of  $E = 20$  kJ/mol. Finally, Brillouin and X-ray scattering by Fioretto et al.<sup>38</sup> reveal a process with  $E = 7.2$  kJ/mol. While the first two experiments were carried out above  $T_g$  the last one was done between 30 and 330 K. The reported activation energies are within the range of the ones obtained in our study; therefore, we are inclined to believe that same  $\gamma$ -process is probed. Using light scattering (gigahertz range,  $T > T_g$ ), Ding et al.<sup>31</sup> investigated one of the polybutadiene samples studied here (PB-25000). They found a fast process in addition to the  $\alpha$ -process, which cannot be identified as the  $\beta$ -process because the latter has already merged with the  $\alpha$ -process in this temperature range. The reported activation energy ( $E = 15$  kJ/mol<sup>31</sup>) is close to than the one we find ( $E = 17.5$  kJ/mol). A straight line interpolates well the time constants obtained from LS and DS

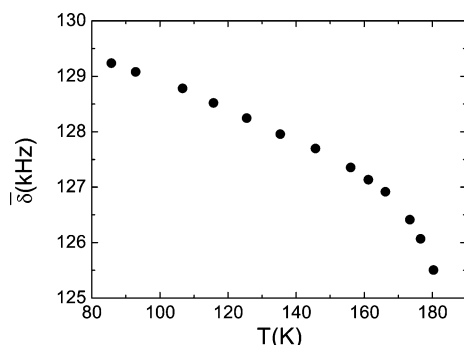


**Figure 10.** Spectral width vs temperature  $T$  for 1,4-polybutadiene- $d_6$  ( $M_w = 80\,000$  g/mol) (spectrum measured with the solid-echo pulse delay  $t_p = 20\,\mu\text{s}$ ).

(cf. Figure 8), suggesting that their Arrhenius dependence on temperature is preserved from the glassy state to the melt.

Most of the authors ascribe the  $\gamma$ -process to conformational motions in the polymer chain. For example, Ding et al.<sup>31</sup> proposed that it originates from a rotation of the  $-\text{H}_2\text{C}-\text{CH}=\text{}$  bond in the backbone of the polymer, explicitly: “fast counterrotation around the double bond allows the double bond to hop without disturbing other monomers along the chain”. Since in all cases the experiments were not directly probing a specific bond, the statements concerning the provenance of the  $\gamma$ -process remained somewhat speculative.

NMR experiments can estimate the angular amplitude of molecular motion (cf. eq 1). Given a motion faster than  $1/\delta$ , solid-echo spectra should yield an averaged spectral width  $\bar{\delta}$ . Actually, as indicated in Figure 10,  $\bar{\delta}$  shows a significant dependence on temperature. The molecular weight of the sample used in the NMR experiments (80 000 g/mol) is close to that of a sample used in DS found to belong to the  $\gamma_A$ -PB class (PB-87000). According to the DS results, at  $T_g$ ,  $\tau_\gamma \approx 10^{-9}$  s  $\ll 1/\delta \approx 10^{-5}$  s is found for the time constants of the  $\gamma$ -process, and thus, as said, a motionally averaged spectral width  $\bar{\delta}$  is expected for the solid echo spectrum. On the other hand, at the lowest temperature ( $T \sim 80$  K) the relation  $\tau_\gamma \gg 1/\delta \approx 10^{-5}$  s holds (cf. Figure 8) so that a spectral width  $\delta$  typical of a rigid body is expected. Assuming that the change of the spectral width depicted in Figure 10 is entirely caused by the  $\gamma$ -process, we can estimate the upper bound of the angular amplitude of molecular motion within a simple cone model by applying eq 3. More precisely, presuming that during the  $\gamma$ -process the  $\text{C}-^2\text{H}$  bond of the PB molecule describes a cone, we found as an upper limit for the semiangle of the cone  $\chi \approx 8^\circ$ . Hence, a highly restricted motional process is responsible for the  $\gamma$ -process, which is not easily associated with conformational changes of the polymer chain, which imply large angle motion. However, we emphasize that a behavior similar to that shown in Figure 10 is found in many glass formers even when fast secondary processes are absent. Thus, much more likely than assuming effects from a  $\gamma$ -process, the continuous change of  $\bar{\delta}$  with temperature may be connected to vibrational phenomena. As a consequence, the angle  $\chi$  is expected to be even smaller than  $8^\circ$ .

The angular amplitude of the  $\gamma$ -process can also be estimated from the DS spectra. As shown by Döss et al.,<sup>42</sup> applying the cone model and making the approximation  $\Delta\epsilon_\gamma, \Delta\epsilon_\beta \ll \Delta\epsilon_\alpha$ , one obtains for the cone

semiangle  $\chi$ :  $\sin(\chi) \propto (\Delta\epsilon_\gamma/\Delta\epsilon_\alpha)^{1/2}$ . By using the amplitude of the relaxation peaks multiplied with its width as an estimate for  $\Delta\epsilon_\gamma$  and  $\Delta\epsilon_\alpha$ , we get  $\chi_{\text{DS}} \approx 11^\circ$  for the sample PB-87000 (that has its  $M_w$  close to the one measured by NMR), which again reflects a small-amplitude process. However, one should keep in mind that the DS relaxation strength of the investigated polymers varies strongly; therefore, also the estimated angular amplitude of the motion may be larger for some (an extreme case is PB-11400).

For the sample PB-25000 (measured by LS) we can conclude from the DS data that the angular amplitude of the molecular motion for the  $\gamma$ -process is very small, comparable to that of PB-87000. On the other hand, the LS data<sup>31</sup> from the melt suggest motion with a larger angular amplitude (as deduced from the intensity of the  $\gamma$ -peak compared to that of the  $\alpha$ -peak). Then, to resolve this discrepancy, it may be that the  $\gamma$ -process exhibits a similar property as the  $\beta$ -process: its relaxation strength increases above  $T_g$  but is small and essentially constant below, as indicated by our NMR and DS experiments. In the case of the  $\beta$ -process this was concluded from NMR,<sup>21,22</sup> dielectric spectroscopy,<sup>8</sup> and neutron scattering experiments.<sup>12</sup> Though, similar to the  $\beta$ -process, a small percent of molecules having a large angular amplitude cannot be ruled out. Again, is not easy to explain such a behavior by a simple conformational change, and it points into the direction that also the  $\gamma$ -process couples to structural relaxation ( $\alpha$ -process). Moreover, the observation that a guest molecule (benzene) participates in the  $\gamma$ -process as well as in the  $\beta$ -process demonstrates that secondary processes in glasses cannot be described by single particle motion.

While the origin of the  $\gamma$ -process in PB remains to be unraveled, this paper proves without doubt its presence and puts strong restraints on any model chosen to rationalize it. We emphasize once again that the strength of the  $\gamma$ -process varies strongly in the different polymers studied. However, there is no clear-cut relationship between the manifestation of the  $\gamma$ -process and the molecular weight or concentration of the building units though two groups with essentially the same time constants are found. It is difficult to understand why the small-amplitude motion ( $\gamma$ -process) varies strongly in the various polymers. Although the content of cis, trans, and vinyl units is similar in the high molecular weights samples (see Experimental Details), it still may be possible that sequence distribution is different in a considerable way, and this may change significantly the local microstructure in the glass ( $T < T_g$ ), thus influencing the relaxation strength of the  $\gamma$ -process.

**Acknowledgment.** We thank A. P. Sokolov (Akron, OH), who was kind to provide us the sample PB-25000, and to D. Richter (Jülich, Germany) for the sample PB- $d_6$ . We highly appreciate the help of J. Gmeiner, J. Senker, and Olek Tok (all from Uni. Bayreuth, Germany) for the  $^{13}\text{C}$  NMR measurements and analysis of the data. The financial support of the Deutsche Forschungsgemeinschaft is gratefully acknowledged.

## Appendix. $^{13}\text{C}$ NMR Measurements

Looking for a possible explanation of the different manifestation of the  $\gamma$ -process, we determined the chemical structure of the chosen PB polymers, in terms of the cis, trans, and vinyl content.  $^{13}\text{C}$  NMR spectra were measured and analyzed as proposed by Sato et al.<sup>53</sup>

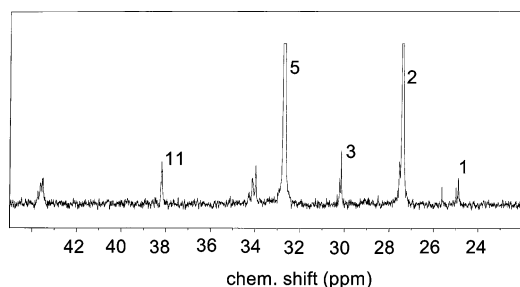


**Figure 11.**  $^{13}\text{C}$  spectrum for PBD-11500. The peaks are identified according to Sato et al.<sup>53</sup>

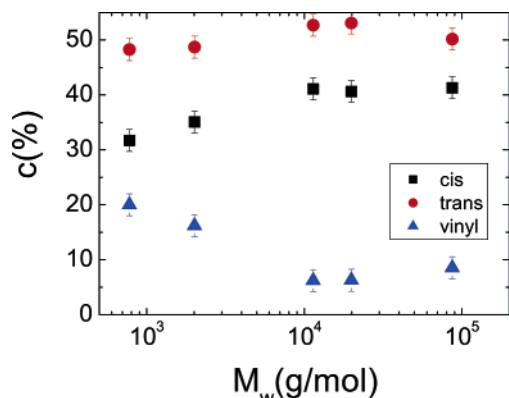


**Figure 12.** Concentration of cis, trans, and vinyl units in the polybutadiene samples.

A typical spectrum is presented in Figure 11 where the peaks are identified according to their chemical shift presented in Table 3 in Sato et al.<sup>53</sup> Using eqs 1–8 in the before-mentioned reference and the integral of the numbered peaks, one can estimate the content of cis, trans, and vinyl units. The results for our samples are displayed in Figure 12. Clearly, a systematic change occurs with molecular weight. However, interpreting  $^{13}\text{C}$  spectra under  $^1\text{H}$  decoupling conditions, some care has to be taken. Because of cross-relaxation effects, some of the NMR intensities may be distorted. However, since quite similar PB spectra were recorded, it means that these effects are very similar for all spectra and do not change the conclusion concerning the molecular dependence.

## References and Notes

- McCrum, N. G.; Read, B. E.; Williams, G. In *Anelastic and Dielectric Effects in Polymeric Solids*; Dover Publications: New York, 1991.
- Kremer, F.; Schönhals, A. In *Broadband Dielectric Spectroscopy*; Springer: Berlin, 2003.
- Böttcher, C. I. F.; Borderwijk, P. In *Theory of Electric Polarization*; Elsevier: Amsterdam, 1978; Vol. 2.
- Williams, G.; Watts, D. C. *Trans. Faraday Soc.* **1971**, 67, 1971.
- Schmidt-Rohr, K.; Spiess, H. W. In *Multidimensional Solid-State NMR and Polymers*; Academic Press: New York, 1994.
- Böhmer, R.; Diezemann, G.; Hinze, G.; Rössler, E. *Prog. Nucl. Magn. Reson. Spectrosc.* **2001**, 42, 191.
- Moreno, A. J.; Alegria, A.; Colmenero, J.; Prager, M.; Grimm, H.; Frick, B. *J. Chem. Phys.* **2001**, 115, 8958.
- Kudlik, A.; Benkhof, S.; Blochowicz, T.; Tschirwitz, C.; Rössler, E. *J. Mol. Struct.* **1999**, 479, 201.
- Johari, G. P.; Goldstein, M. *J. Chem. Phys.* **1970**, 53, 2372.
- Hansen, C.; Richert, R. *Acta Polym.* **1997**, 48, 484.
- Deegan, R. D.; Nagel, S. R. *Phys. Rev. B* **1995**, 52, 5653.
- Arbe, A.; Richert, D.; Colmenero, J.; Farago, B. *Phys. Rev. E* **1996**, 54, 3853.
- Casalini, R.; Ngai, K. L.; Robertson, C. G.; Roland, C. M. *J. Polym. Sci., Part B: Polym. Phys.* **2000**, 38, 1841.
- Roland, C. M.; Schroeder, M. J.; Fontanella, J. J.; Ngai, K. L. *Macromolecules* **2004**, 37, 2630.
- Schmidt-Rohr, K.; Kulik, A. S.; Beckham, H. W.; Ohlemacher, A.; Pawelzik, U.; Boeffel, C.; Spiess, H. W. *Macromolecules* **1994**, 27, 4733.
- Kulik, A. S.; Radloff, D.; Spiess, W. H. *Macromolecules* **1994**, 27, 3111.
- Kulik, A. S.; Beckham, H. W.; Schmidt-Rohr, K.; Radloff, D.; Pawelzik, U.; Boeffel, C.; Spiess, H. W. *Macromolecules* **1994**, 27, 4746.
- Wagner, H.; Richert, R. *J. Non-Cryst. Solids* **1998**, 19, 242.
- Böhmer, R.; Hinze, G.; Jörg, T.; Qi, F.; Sillescu, H. *J. Phys.: Condens. Matter* **2000**, 12, A383.
- Vogel, M.; Rössler, E. *J. Phys. Chem.* **2000**, 104, 4285.
- Vogel, M.; Rössler, E. *J. Chem. Phys.* **2001**, 114, 5802.
- Vogel, M.; Rössler, E. *J. Chem. Phys.* **2001**, 115, 10883.
- Vogel, M.; Tschirwitz, C.; Schneider, G.; Koplin, C.; Medick, P.; Rössler, E. *J. Non-Cryst. Solids* **2002**, 307–310, 326.
- Böhmer, R.; Hinze, G.; Jörg, T.; Qi, F.; Sillescu, H. *J. Phys.: Condens. Matter* **1999**, 11, 1.
- Ngai, K. L.; Paluch, M. *J. Chem. Phys.* **2004**, 120, 857.
- Blochowicz, T.; Rössler, E. A. *Phys. Rev. Lett.* **2004**, 92, 225701-1-4.
- Ngai, K.; Capaccioli, S. *Phys. Rev. E* **2004**, 69, 031501.
- Beiner, M.; Kahle, S.; Hempel, E.; Schröter, K.; Donth, E. *Macromolecules* **1998**, 31, 8973.
- Olsen, N. B. *J. Non-Cryst. Solids* **1998**, 235–237, 399.
- Paluch, M.; Roland, C. M.; Pawlus, S.; Ziolo, J.; Ngai, K. L. *Phys. Rev. Lett.* **2003**, 91, 115701.
- Ding, Y.; Novikov, V. N.; Sokolov, A. P. *J. Polym. Sci., Part B: Polym. Phys.* **2004**, 42, 994.
- Aouadi, A.; Lebon, M. J.; Dreyfus, C.; Strube, B.; Steffen, W.; Patkowski, A.; Pick, R. M. *J. Phys.: Condens. Matter* **1997**, 9, 3803.
- Richter, D.; Zorn, R.; Frick, B.; Fetters, L. J.; Farago, B. *Phys. Rev. Lett.* **1992**, 68, 71.
- Gee, R. H.; Boyd, R. H. *J. Chem. Phys.* **1994**, 101, 8028.
- Kim, E.-G.; Mattice, W. L. *J. Chem. Phys.* **2002**, 117, 2389.
- Götze, W. *J. Phys.: Condens. Matter* **1999**, 11, A1.
- Zorn, R.; Arbe, A.; Colmenero, J.; Frick, B.; Richter, D.; Buchenau, U. *Phys. Rev. E* **1995**, 52, 781.
- Fioretto, D.; Masciovecchio, C.; Mattarelli, M.; Monaco, G.; Palmieri, L.; Ruocco, G.; Sette, F. *Philos. Mag. B* **2002**, 82, 273.
- Pake, G. E. *J. Chem. Phys.* **1948**, 16, 327.
- Spiess, H. W. *J. Chem. Phys.* **1980**, 72, 6755.
- Vogel, M.; Rössler, E. *J. Magn. Reson.* **2000**, 147, 43.
- Döss, A.; Paluch, M.; Sillescu, H.; Hinze, G. *Phys. Rev. Lett.* **2002**, 88, 095701.
- Döss, A.; Paluch, M.; Sillescu, H.; Hinze, G. *J. Chem. Phys.* **2002**, 117, 6582.
- Blochowicz, T.; Kudlik, A.; Benkhof, S.; Senker, J.; Rössler, E.; Hinze, G. *J. Chem. Phys.* **1999**, 110, 12011.
- Rössler, E.; Sokolov, A. P.; Eiermann, P.; Warschewske, U. *Physica A* **1993**, 201, 237.
- Wagner, H.; Richert, R. *J. Phys. Chem. B* **1999**, 103, 4071.
- Schnauss, W.; Fujara, F.; Sillescu, H. *J. Chem. Phys.* **1992**, 97, 1378.
- Dries, Th.; Fujara, F.; Kiebel, M.; Rössler, E.; Sillescu, H. *J. Chem. Phys.* **1988**, 88, 2139.
- Lusceac, S. A.; LeQuellerc, C.; Koplin, C.; Medick, P.; Vogel, M.; Alba-Simionesco, C.; Rössler, E. A. *J. Phys. Chem. B* **2004**, 108, 16601.
- Schneider, U.; Brand, R.; Lunkenheimer, P.; Loidl, A. *Phys. Rev. Lett.* **2000**, 84, 5560.
- Adichtchev, S.; Blochowicz, T.; Gainaru, C.; Novikov, V. N.; Rössler, E. A.; Tschirwitz, C. *J. Phys.: Condens. Matter* **2003**, 15, S835.
- Kanya, T.; Kawaguchi, T.; Kaji, K. *Macromolecules* **1999**, 32, 1672.
- Sato, H.; Takebayashi, K.; Tanaka, Y. *Macromolecules* **1987**, 20, 2418.